

# RAMP DESIGN AND IMPLEMENTATION FOR THE RHIC DEUTERON-GOLD AND POLARIZED PROTON RUNS

J. van Zeijts, A. Marusic, BNL Collider Accelerator Department, Upton, USA\*

## Abstract

The RHIC magnet ramping management system went through a rewrite designed for increased flexibility and inclusion of more magnet specific transfer function and multipole data. The resulting system allows beta\* squeezing on the acceleration ramp or independently at constant dipole field. We describe the ramp design, the major changes in the system, which include unequal species ramping, and show the increased agreement with measured machine parameters. Ramp implementations details are shown for the Deuteron-Gold and the Polarized Proton runs.

## 1 INTRODUCTION

The RHIC ramping software server environment consists of a RampManager, On-Line Models and WFG Managers. The Ramping and Model servers are implemented using the CDEV generic server architecture which offer a mature environment for server development while maintaining the same user API as regular control system calls. The server code base consists of about 100000 lines of C++.

The magnet settings on a ramp are organized in time as a set of ‘stepstones’, interpolation of the strengths in between stepstones is either linear or cubic splines, depending on the magnet type. Ramps and Stepstones are accessible as named CDEV devices, and offer access to set/get/monitor magnet values and get/monitor the associated optics parameters. In addition the model server allows setting of machine tunes at each stepstone.

All control room applications that need optics data retrieve this from the on-line model. This includes the RHIC injection application, Ring orbit correction, the AC-dipole optics analysis application, the Decoupling Tune Scan application, Luminosity scanning application and other applications and scripts.

## 2 RAMP DESIGN

### 2.1 Energy Ramp

A RHIC ramp is specified by the dependence of  $B\rho(\text{ring}, t)$ , which determines the energy of the beam, and  $\beta^*(\text{ring}, ip, t)$ , which determines the beam size at each interaction-point (IP). Taken together these settings determines the current in each magnet, and conversely in each powersupply. The time dependance of  $B\rho$  is constrained by the main dipole and quadrupoles ramping speed. The

dipole current and its time derivative are related to the dipole angle as:

$$\begin{aligned} \alpha \times B\rho &= Bdl = I \times TF(I) \\ \alpha' \times B\rho + \alpha \times B\rho' &= I' \times (TF(I) + I \times TF'(I)) \end{aligned}$$

where  $Bdl$  is the integrated magnetic field strength and  $TF(I)$  is the ‘Transfer-Function’ for the magnet. Typical values for  $TF(I) = 0.0068\text{Tm/A}$ ,  $\alpha = 38\text{mrad}$ , and  $I'_{max} = 24\text{A/s}$  give a  $B\rho'_{max} \sim 4\text{Tm/s}$ , where we assume the dipole angle does not change. This maximum ramp speed needs to be approached smoothly to avoid power supply voltage spikes, for that reason the  $B\rho(t)$  is specified as a set of cubic polynomials. In order to minimize tracking errors in the nested power supply scheme, we choose the initial  $B\rho(t)$  to start with zero first and second order derivatives. Figure 1 shows a typical picture of  $B\rho$  and its derivatives.

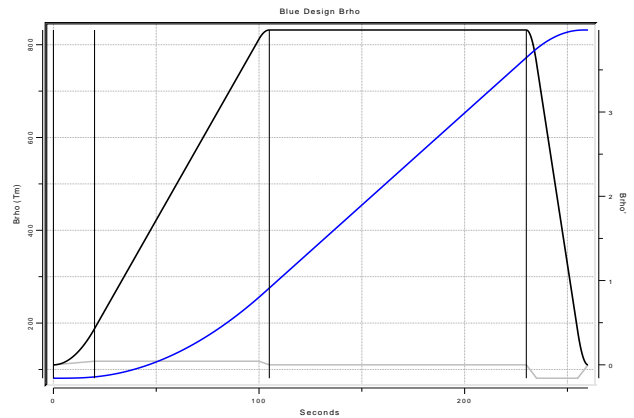


Figure 1:  $B\rho(t)$  (Blue) and derivatives

### 2.2 $\beta^*$ Ramp

Physics limitations for the  $\beta^*$  squeeze include beam-size considerations; since the maximum beam size scales with  $1/\beta^* \times 1/(\beta\gamma)$ , care should be taken to not squeeze the beam faster than we accelerate. Other limitations come from insertion power-supplies range and voltage constraints, which determine how fast, and how much we can squeeze. Within these limits there is some flexibility in choosing the time dependance of the  $\beta^*$  functions, we can use the flexibility to, for instance, move 1 IP to a lower  $\beta^*$  along the last part of the ramp. Again the functional form of the  $\beta^*(t)$  is as a set of cubic polynomials, where the value

\* Work performed under the auspices of the US Department of Energy

and the first derivative are matched at each intersection to enforce smooth power-supply currents, and voltage.

### 2.3 FY03 Ramps

For the Deuteron-Gold (d/Au) ramps the beam is squeezed down while we accelerate for 240 seconds, the  $B\rho(t)$  and  $\beta^*(t)$  are shown in Figure 3. This choice was driven by the requirements of  $\beta^* = 10m$  at injection, and  $\beta^* = 5m$  for optimal transition optics. For Polarized Protons (pp) we inject above transition, and the pp ramp consists of constant  $\beta^*$  acceleration to flattop  $B\rho$  for the first 140 seconds, and subsequently, starting at 150 seconds, squeezing at fixed  $B\rho$  to the final  $\beta^*$ , see Figure 2. A

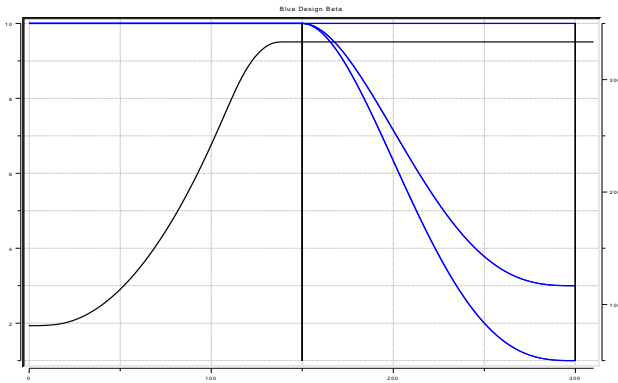


Figure 2: pp Ramp:  $\beta^*(t)$  (Blue) and  $B\rho(t)$  (Black)

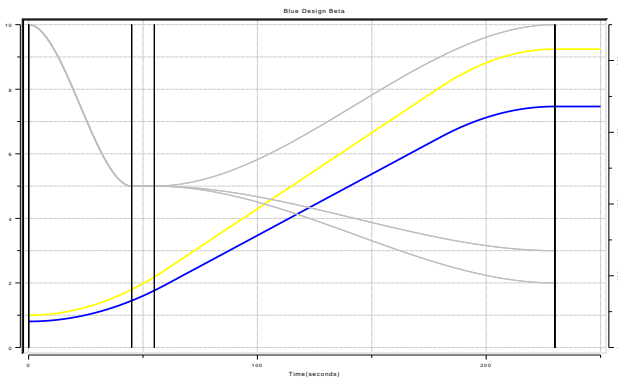


Figure 3: d/Au Ramp:  $\beta^*(t)$  (Grey) and  $B\rho(t)$  (Blue, Yellow)

serendipitous effect of this choice for the pp ramp was to facilitate analysis of optics errors originating from the  $\beta$  squeeze without the complications of a changing  $B\rho$ .

### 2.4 Ramp Controls Implementation

The  $B\rho(t)$  and  $B\rho'(t)$  are programmed in a Wave-Form-Generator (WFG) and send out over the Real-Time-Data-Link (RTDL) at 720Hz for each ring. Each power-supply is programmed with its logically connected magnet strengths

from the stepstones. A 'pseudo-time' generator is programmed to provide a linear time axis at 720Hz on RTDL. All wfg's are triggered by the same starting event, when this event occurs each wfg starts going through its formulas. The logical steps in the formulas, repeated at 720Hz, are

- Read Pseudo-Time and  $B\rho$  from RTDL
- Read Main-Dipole or Main-Quad bus currents from RTDL
- Look up Magnet strength in linear, or cubic-spline table as a function of pseudo-time
- Calculate Magnetic Field strength
- Look up Magnet current in Transfer-Function table
- Subtract Main Bus current(s)
- Send out resulting current over fiber link

The power-supply interface board subtracts the current of the neighbouring wfg and sends the difference signal to the actual hardware.

## 3 ONLINE MODEL

Each optics model at RHIC consists of 2 parts, both containing the same physics and knowledge about the machine, but differing in the setpoints of the magnets. The first is the 'design' model where tunes are set to design values. Each magnet receives its 'design' setting from this model, and modifications of the  $\beta^*$  are done in this model. During commissioning of a ramp, measured tunes are adjusted by introducing 'trim' settings for magnets located only on the main-quad buses. The resulting optics is modeled in the 'trim' model, whose deviation from design is, in some sense, a measure of our understanding about the machine optics.

For the FY02 ramps there was a large tune discrepancy at Injection and partly up the ramp. In the analysis of the optics it was realized that extra quadrupole focussing terms due to dipole  $B_2(I)$  (sextupole) component feed-down where responsible for a large part of the model tune discrepancies. Figure 4 shows the predicted tunes without and with the dipole feed-down, where we used a constant offset along the ramp of  $\Delta x = 2.15mm$ . A significant improvement is seen in the modeled tune separation.

For FY03, the RHIC online model and RampManager have been set up with individual Transfer-Functions for each quadrupole. Tune discrepancies are now largely confined to the constant  $B\rho$  part of the ramp where the main features of the remaining tune differences is the negative tune swing during the squeeze. In the next section we propose a possible explanation for this effect.

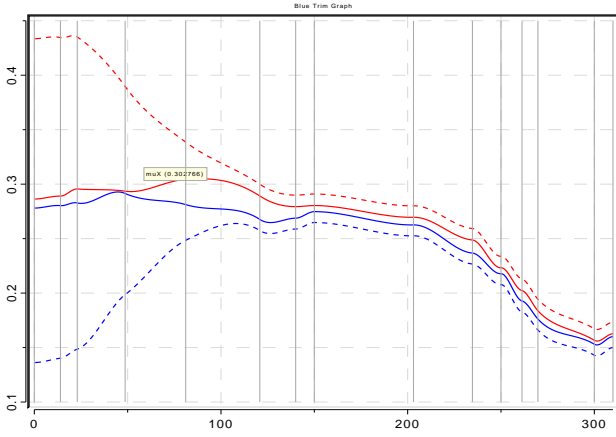


Figure 4: Blue Tunes: No  $B_2$  feed-down (Dashed), with  $B_2$  feed-down correction (Solid) assuming  $\Delta x = 2.15mm$

### 3.1 Modified Transfer-Functions

Here we allow errors in Transfer-Functions for the main-dipoles and the main quadrupoles. Since we have a limited set of data, we group the changes in three sets: one change for the main-dipole  $\frac{\Delta B\rho}{B\rho}$ , one change for all quads only on the main-quad busses  $\frac{\Delta FD}{FD}$ , and one change for all other quads, namely those in the IP. This last group is split up in two close numbers for fine-tuning  $\frac{\Delta F}{F}$ ,  $\frac{\Delta D}{D}$ .

Modifying the main-dipole transfer-functions gives an effect on  $B\rho$  as shown below:

$$\frac{\Delta B\rho}{B\rho} = -\frac{\Delta\alpha}{\alpha} + \frac{\Delta I_d}{I_d} + \frac{\Delta T_d}{T_d} \quad (1)$$

and the integrated quadrupole strengths are modified as follows:

$$\frac{\Delta KL}{KL} = -\frac{\Delta B\rho}{B\rho} + \frac{\Delta I_q}{I_q} + \frac{\Delta T_q}{T_q} \quad (2)$$

We assume no powersupply errors:  $\Delta I = 0$ , and no angle errors:  $\Delta\alpha = 0$ .

Table 1:  $\frac{\Delta T}{T}$

What	Blue	Yellow
$\frac{\Delta B\rho}{B\rho}$	0.00165	0.0017
$\frac{\Delta FD}{FD}$	-0.0037	-0.0047
$\frac{\Delta F}{F}$	0.00455	0.0045
$\frac{\Delta D}{D}$	0.0045	0.0044

Choosing the number in Table 1 we recalculate the optics along the ramp, and at store. Figures 5. 6 show the model tunes, and we see that we can reach excellent agreement with the measured tunes. As extra evidence we show turn-by-turn AC dipole phase-advance data that is much better explained with our modified TF model (Figure 7).

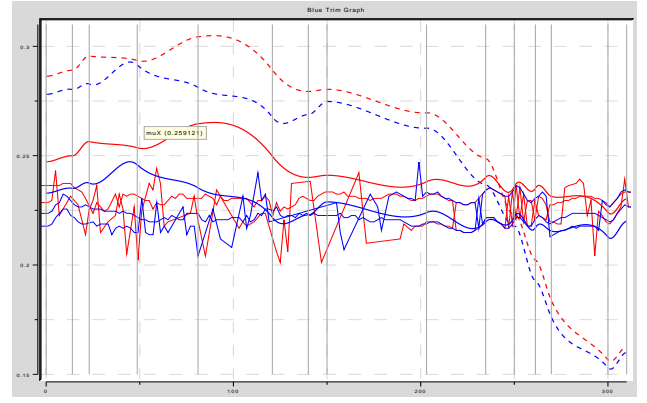


Figure 5: Blue Tunes: Model (Dashed), with TF Correction (Solid), and Measured

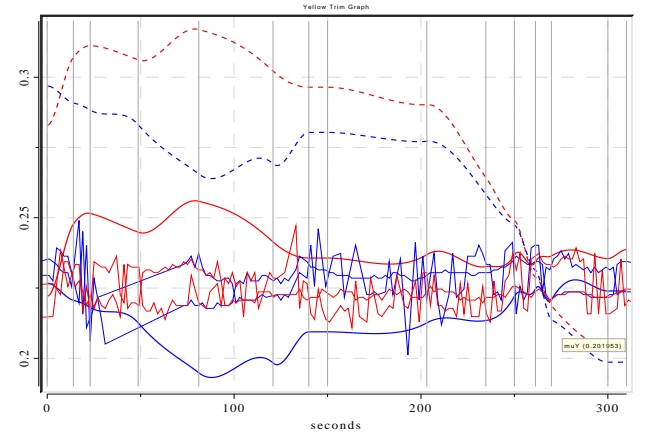


Figure 6: Yellow Tunes: Model (Dashed), with TF Correction (Solid), and Measured

## 4 SUMMARY

We have suggested corrections in magnet transfer-functions which greatly improve the agreement between the model and measured machine. The corrections are based on pp ramp measurements at currents of  $\approx 2000$  Amps and below. The corrections need to be verified, and most likely updated, for currents up to the Au store conditions. We are looking forward to confirming this hypothesis on the upcoming FY04 ramps. If the predictions works out further squeezing below  $\beta^* = 1$  could be considered.

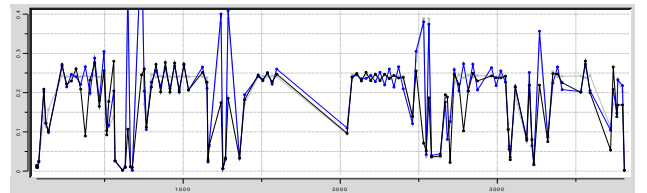


Figure 7: AC Dipole Blue Vertical Phase-Advance Design (Grey), Predicted (Blue), Measured (Black)